J. Fluid Mech. (1992), *vol.* 244, *pp.* 55–78

Propagation of nonlinear acoustic waves in a tunnel with an array of Helmholtz resonators

By N. SUGIMOTO

Department of Mechanical Engineering, Faculty of Engineering Science, University of Osaka, Toyonaka, Osaka 560, Japan

(Received 28 May 1991 and in revised form 11 April 1992)

It is proposed that an array of Helmholtz resonators connected to a tunnel in its axial direction will suppress the propagation of sound generated by a travelling train and especially the emergence of shock waves in the far field. Under the approximation that the resonators may be regarded as continuously distributed, quasi-one-dimensional formulation is given for nonlinear acoustic waves by taking account of not only the resonators but also the wall friction due to the presence of a boundary layer and the diffusivity of sound. For a far-field propagation, the spatial evolution equation coupled with the equation for the response of the resonator is then derived. The linear dispersion relation suggests that the resonators, if appropriately designed, enhance the dissipation and give rise to the dispersion as well. By solving initial-value problems for the evolution equation, the array of resonators is proved to be very effective in suppressing shock waves in the far field. The resonators themselves fail to counteract shock waves once formed, but rather prevent their emergency by rendering acoustic waves dispersive. By this dispersion, it becomes possible, in a special case, for an acoustic soliton to be propagated in place of a shock wave.

1. Introduction

It is likely that in future high-speed trains will have to travel inside tunnels because of the environmental noise problem and the weather problem. Tunnels will then become unprecedentedly long and many acoustic problems in tunnels will have to be overcome. This may open up a new field to be categorized as a 'tunnel acoustics'.

Pressure disturbances generated by a travelling train are propagated along a tunnel in the form of sound. As the tunnel plays the role of a waveguide for the sound, it is transmitted far down without geometrical spreading. While the intensity depends on the ratio of the cross-sectional area of the train to that of the tunnel, the faster the train travels, the more intense is the sound generated. Thus it is possible, in a long tunnel, for shock waves to emerge unexpectedly far down the tunnel, even if the speed of the train is well below the sound speed.

In considering a sound field generated, it becomes important to distinguish between the near field and the far field of the train. In the near field, many sources of sound are identified which are attributable to the geometry of the train and the tunnel. In this field, a very complicated sound field of a three-dimensional nature is built up, involving a wide range of frequencies. As the distance from the train increases, however, the high-frequency components involved will fade out owing to dissipation and eventually almost one-dimensional propagation along the tunnel will remain.

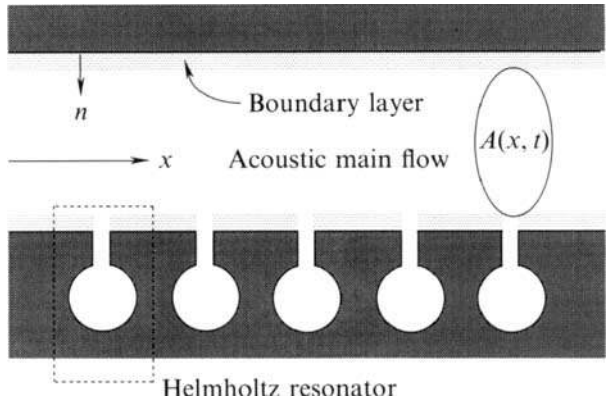

FIGURE 1. Tunnel with an array of Helmholtz resonators where the x-axis is taken along the axis of the tunnel and the n axis is chosen inward normal to the tunnel wall; $A(x,t)$ represents a cross-sectional area of the acoustic main flow excluding a thin boundary layer and the vicinity of the orifice of a resonator but A is almost equal to the area of the whole geometrical cross-section of the tunnel.

This far-field propagation is characterized by the length of the train l, its speed U, the diameter of the tunnel D and the ratio of the cross-sectional area of the train to that of the tunnel χ. A typical frequency of the pressure disturbances is estimated to be a_0/l to a_0/D, a_0 being the sound speed, but the magnitude of the pressure disturbances depends on how the train is accelerated. A maximum magnitude would be attained, as an extreme case, when the train suddenly sets in motion with a constant speed U. To estimate it, the train is regarded as the one-dimensional dipole of strength $\rho_0 \chi l U$ per unit cross-sectional area of the tunnel where ρ_0 is the density of air. Then the linear acoustic theory estimates that the maximum magnitude relative to the atmospheric pressure is of order $\chi M/(1-M)$ where $M(= U/a_0)$ is the Mach number of the train ($M < 1$). Although this result will overestimate the real value, it is worth noting that for a small value of M, the magnitude is proportional to M rather than M^2 and that as M approaches unity, it tends to diverge. As a typical example, suppose that a train of length 100 m be accelerated suddenly to travel with speed 150 m/s (540 km/h) in a tunnel of diameter 10 m. The typical frequency is estimated to a few Hertz to 10 Hz, while the magnitude is estimated for $\chi = 0.1$ to be 0.08 (corresponding to 172 dB in the sound pressure level). Since such an infrasound is subjected to less dissipation, it is highly probable that the nonlinearity accumulates in the course of propagation to give rise eventually to shock waves.

In order to avoid their emergence, it is proposed to connect many Helmholtz resonators in array to a tunnel (as shown in figure 1). Each resonator consists of a large cavity and a throat through which the cavity is connected to the tunnel (see figure 2). For simplicity, identical resonators are assumed to be connected with equal axial spacing, d. Let the number of resonators per characteristic wavelength Λ be large, i.e. $\Lambda/d \gg 1$, so that the resonators may be regarded as continuously distributed. Each resonator acts as an agent giving rise to reflection of the acoustic waves in the tunnel. The degree of reflection is controlled by the ratio of the volume of the cavity V to that of the tunnel per spacing d, i.e. V/Ad. To the extent that V/Ad remains small, the reflection is considered small also. This paper considers a case of small reflection such that neighbouring resonators respond almost in unison to the local pressure disturbances in the tunnel and an interaction between those resonators is ignored.

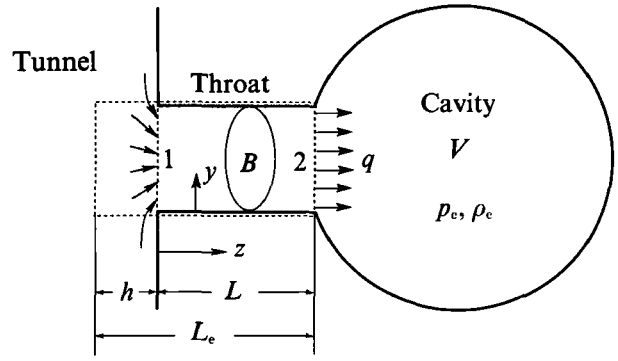

FIGURE 2. Helmholtz resonator with a cavity of volume V and a throat of length L; the y-axis is chosen inward normal to the throat wall while the z-axis is taken along the throat with its origin at orifice 1 on the tunnel side.

To pursue a far-field propagation quantitatively, dissipation must be taken into account. The dissipation results from both the diffusivity of sound itself and the wall friction through the presence of a boundary layer. For propagation of infra-sound, the former effect is negligibly small compared with the latter one. The wall friction exhibits a hereditary (memory) effect so that it accumulates in the course of propagation to influence globally the far-field behaviour. In contrast, the diffusivity of sound becomes important only if shock waves appear, but very locally in a thin shock layer.

In what follows, formulation is first given, in §2, for quasi-one-dimensional propagation of nonlinear acoustic waves in the tunnel with the array of Helmholtz resonators. Dissipative effects due to the wall friction and to the diffusivity of sound are taken into account in general, while the response of the resonator is included within the linear theory. As the magnitude of pressure disturbances tends to be high, the nonlinear response comes into play. For this case, the nonlinear theory for the response of the resonator is developed in the Appendix. A spatial evolution equation coupled with the equation of the response of the resonator is derived in §2. On the basis of these equations, in §3, local properties of a discontinuous solution are examined and then some initial-value problems are solved to see the effectiveness of the array in suppressing the emergence of shock waves. There is a brief discussion on a special case in which an acoustic soliton rather than a shock wave can be propagated.

2. Formulation of the problem

In the following, the tunnel is regarded as a straight pipe of infinite length having a smooth interior surface, to which a single array of Helmholtz resonators is connected (as shown in figure 1). A cross-section of the tunnel is assumed to be axially uniform but it may be of any shape other than circular, as long as its boundary is smooth. Let the identical resonator be connected to the tunnel with the axis of the throat normal to that of the pipe. Each resonator may be positioned arbitrarily along the periphery of the tunnel, if the axial spacing is kept equal and narrow.

To formulate the problem, at first, the acoustic main flow in the tunnel is defined as that excluding a thin boundary layer adjacent to the tunnel wall and the vicinity of orifices from the resonators. In this region, the assumption of quasi-one-dimensional flow can be exploited. Thus, let all physical quantities for the main flow

be a sum of the averaged quantities over its cross-section and the small 'deviations' from them. Of course, the deviations result from the axial non-uniformity in the boundary-layer thickness and the response of the resonator. The guiding principle for the formulation is to take account of all terms up to the first order of the deviations. However, because the viscous and thermal effects are small in the main flow, even the first-order deviation, if multiplied by the viscosity or the thermal conductivity, is neglected.

Following this principle, the equation of continuity is given by

$$\frac{\partial \rho}{\partial t}+\frac{\partial}{\partial x}(\rho u)=\frac{1}{A}\oint \rho v_{\mathrm{n}}\,\mathrm{d}s, \tag{2.1}$$

where ρ and u denote, respectively, the mean values of the density and the axial velocity of the gas (i.e. air) averaged over the cross-section of the main flow with its area $A = A(x,t)$, x and t being the axial coordinate and the time. The right-hand side is the first-order deviation which represents the mass flux through the edge of the boundary layer and the orifices of the resonators, v_{n} being the small deviation of the velocity inward normal to the boundary of the cross-section of the main flow and $\mathrm{d}s$ the small line element along it. In deriving (2.1) by averaging the three-dimensional equation of continuity, the variations of A with respect to x and t are small and of comparable order to the deviations.

Within the same approximation, the equation of motion, i.e. Navier–Stokes equation in the axial direction of the tunnel takes simply the one-dimensional form:

$$\frac{\partial u}{\partial t}+u\frac{\partial u}{\partial x}=-\frac{1}{\rho}\frac{\partial p}{\partial x}+\frac{1}{\rho}(\tfrac{4}{3}\mu+\mu_{\mathrm{v}})\frac{\partial^2 u}{\partial x^2}, \tag{2.2}$$

where p is the mean pressure; μ and μ_{v} are, respectively, the coefficients of the shear and bulk viscosities. Throughout this paper, such material constants, as well as the thermal conductivity below, are assumed to be constant. With the axis of the throat normal to that of the tunnel, the resonators do not contribute to the momentum flux in the axial direction.

The equation of energy also takes the one-dimensional form, as long as the thermal effect is assumed to be small compared to the viscous one. Thus it follows that

$$\rho T\left(\frac{\partial S}{\partial t}+u\frac{\partial S}{\partial x}\right)=k\frac{\partial^2 T}{\partial x^2}+(\tfrac{4}{3}\mu+\mu_{\mathrm{v}})\left(\frac{\partial u}{\partial x}\right)^2, \tag{2.3}$$

where T and S denote, respectively, the mean temperature and the entropy, k being the thermal conductivity. In addition to these equations, the equation of state for the ideal gas is assumed for air, i.e. $p = \mathscr{R}\rho T$ where $\mathscr{R}$ is the gas constant. Then the pressure can alternatively be expressed in terms of ρ and S as follows:

$$\frac{p}{p_0}=\left(\frac{\rho}{\rho_0}\right)^{\gamma}\exp\left(\frac{S-S_0}{c_v}\right), \tag{2.4}$$

with $\gamma = c_p/c_v$, where c_p and c_v are specific heats at constant pressure and volume, respectively; the subscript '0' for p_0, ρ_0, S_0 and T_0 in (2.5) below implies the respective equilibrium value.

From (2.1) to (2.4), the effect of resonators as well as that of the boundary layer appear only in the mass flux on the right-hand side of (2.1). In other respects, the system of equations is the same as that in the one-dimensional case. Thus a procedure to develop the nonlinear theory for acoustic waves subjected to the weak dissipative

effect follows in the same way, except for the effect of resonators, as demonstrated in previous papers (Lighthill 1956; Chester 1964; Sugimoto 1989). Hence, the description of this process is limited here to the minimum.

Both weak effects of nonlinearity and dissipation are measured by the acoustic Mach number ϵ and the acoustic Reynolds number Re:

$$\frac{u_0}{a_0} = \epsilon \ll 1, \quad \frac{\omega\nu}{a_0^2} = \frac{1}{Re} \ll 1,$$

where u_0 and a_0 denote, respectively, a characteristic velocity of the gas induced by the acoustic waves and the linear sound speed, while ω and ν denote a characteristic angular frequency and the kinematic viscosity, respectively. In passing, the magnitude of pressure disturbance is estimated to be $\gamma\epsilon$ by the linear theory. The following analysis takes full account of nonlinearity except for the dissipative terms for which only linear effects are retained. By this approximation, the adiabatic relation is modified to include the small change in the entropy. Then (2.3) may be approximated by

$$\rho_0 T_0 \frac{\partial S}{\partial t} = k \frac{\partial^2 T}{\partial x^2}. \tag{2.5}$$

Using the adiabatic relation (2.4) with $S = S_0$, together with the equation of state, $(T-T_0)/T_0$ is given in terms of the variation of $(\rho-\rho_0)/\rho_0$. Further, using the first-order relation of (2.2), i.e. $\rho_0 \partial u/\partial t = -a_0^2 \partial\rho/\partial x$ with $a_0^2 = \gamma p_0/\rho_0$, the entropy change is related to u by

$$\frac{\partial S}{\partial x} = -\frac{(\gamma-1)k}{\gamma p_0} \frac{\partial^2 u}{\partial x^2}. \tag{2.6}$$

The pressure gradient in (2.2) takes account of this entropy change in addition to the density change:

$$\frac{\partial p}{\partial x} = \frac{\partial p}{\partial \rho}\bigg|_S \frac{\partial \rho}{\partial x} + \frac{\partial p}{\partial S}\bigg|_\rho \frac{\partial S}{\partial x}. \tag{2.7}$$

Following the standard procedure, ρ in (2.1) and (2,2) is expressed in terms of the local sound speed a defined by $a = [\partial p/\partial\rho)_{S=S_0}]^{\frac{1}{2}} = a_0(\rho/\rho_0)^{\frac{1}{2}(\gamma-1)}$. After some manipulation, it follows that

$$\left[\frac{\partial}{\partial t} + (u \pm a)\frac{\partial}{\partial x}\right]\left(u \pm \frac{2}{\gamma-1}a\right) = \pm\frac{a}{\rho A}\oint \rho v_n \, ds + \nu_d \frac{\partial^2 u}{\partial x^2}, \tag{2.8}$$

with the signs vertically ordered, where $\nu_d\{= \nu[\frac{4}{3} + \mu_v/\mu + (\gamma-1)/Pr]\}$ is the diffusivity of sound and Pr $(= \mu c_p/k)$ the Prandtl number. In order to close (2.8), ρv_n must now be specified by examining the flow in the boundary layer and the response of the resonator.

2.1. *Effect of boundary layer*

An effect of the boundary layer has already been examined by Chester (1964). The boundary layer consists of two layers for the velocity and the temperature. For the first-order deviation of ρv_n in (2.8), it only suffices to linearize the boundary layer around the equilibrium state. Applying the boundary-layer approximation, it immediately follows from the equation of motion normal to the tunnel wall that the pressure in the main flow prevails over the boundary layer. On traversing it, thus, the density and the temperature are subjected to the isobaric change, i.e. $\rho'/\rho_0 = -T'/T_0$ where the sums $\rho+\rho'$ and $T+T'$ represent, respectively, the density and the

temperature in the boundary layer. Upon using these relations together with the first-order relations of (2.1) and (2.2) for the main flow, the equation of motion in the axial direction and that of energy are reduced to the following two heat equations for u' and T':

$$\frac{\partial u'}{\partial t} = \nu \frac{\partial^2 u'}{\partial n^2}, \quad \frac{\partial T'}{\partial t} = \frac{\nu}{Pr} \frac{\partial^2 T'}{\partial n^2}, \tag{2.9a, b}$$

where n designates the coordinate inward normal to the tunnel wall (see figure 1); the sum $u+u'$ represents the axial velocity in the boundary layer. The primed quantities such as u' and T' as well as ρ' above depend not only on x and t but also on n, whereas u, T and ρ depend on x and t only.

Equations (2.9) are to be solved under the following matching condition as $n \to \infty$ between the boundary layer and the main flow and the boundary condition at the tunnel wall $n = 0$:

$$u' \to 0, \quad T' \to 0 \quad \text{as } n \to \infty. \tag{2.10a}$$

$$u' = -u, \quad T' = T_0 - T \quad \text{at } n = 0, \tag{2.10b}$$

where the non-slip and isothermal conditions are imposed at the tunnel wall. It is straightforward to solve (2.9) under (2.10) by employing, for example, the method of Fourier transform with respect to time (Sugimoto 1989). When u' and T' are available, the velocity component normal to the edge of the boundary layer, defined as v_b, is obtained by integrating the equation of continuity with respect to n from $n = 0$ to $n = \infty$:

$$\frac{\partial \rho'}{\partial t} + \rho_0 \frac{\partial u'}{\partial x} + \rho_0 \frac{\partial v'}{\partial n} = 0, \tag{2.11}$$

where v' denotes the velocity component normal to the tunnel wall. By doing so, v_b is now evaluated in terms of the axial velocity in the main flow as follows:

$$v_b = \lim_{n \to \infty} v' = C \left(\frac{\nu}{\pi}\right)^{\frac{1}{2}} \int_{-\infty}^{t} \frac{1}{(t-t')^{\frac{1}{2}}} \frac{\partial u(x,t')}{\partial x} \mathrm{d}t' \equiv C \nu^{\frac{1}{2}} \frac{\partial^{-\frac{1}{2}}}{\partial t^{-\frac{1}{2}}} \left(\frac{\partial u}{\partial x}\right), \tag{2.12}$$

with $C = 1 + (\gamma - 1)/Pr^{\frac{1}{2}}$. Note that the deviations in the main flow are small and comparable with v_b. For details of the derivation and definition of the minus half-order derivative, see Chester (1964) and Sugimoto (1989), respectively. Incidentally, the half-order derivative is frequently used in the following. It is defined by differentiating the minus half-order derivative with respect to t once.

$$\frac{\partial^{\frac{1}{2}} u}{\partial t^{\frac{1}{2}}} \equiv \frac{1}{\pi^{\frac{1}{2}}} \int_{-\infty}^{t} \frac{1}{(t-t')^{\frac{1}{2}}} \frac{\partial u(x,t')}{\partial t'} \mathrm{d}t'. \tag{2.13}$$

Furthermore, the derivatives of order $\frac{3}{2}$ and $\frac{5}{2}$ are also used below, which are similarly defined as the ones obtained by differentiating (2.13) once and twice with respect to t, respectively.

2.2. *Effect of Helmholtz resonators*

We now specify the mass flux from the resonators by examining their response. Each resonator consists of a large cavity and a throat of uniform cross-section. The shape of the cavity is arbitrary but its volume is large enough compared with that of the throat. A cross-section of the throat may also be of arbitrary shape as long as its boundary is smooth. Typical dimensions of the cavity and the throat should be much smaller than a characteristic wavelength of the acoustic waves.

For the response of the resonator, the elementary treatment is adopted. Neglecting the motions of the gas inside the cavity, only the conservation of mass is considered:

$$V\frac{\partial \rho_c}{\partial t} = Bq, \tag{2.14}$$

where ρ_c is the mean density of the gas in the cavity of volume V, while B is the area of the whole geometrical cross-section of the throat and q is the mean mass flux density over B into the cavity. A flow in the throat is assumed to be quasi-one-dimensional, just as in the tunnel. In this case as well, an effect of dissipation appears in the form of the friction through a thin boundary layer at the throat wall. Since the situation is the same as that in the tunnel, the same system of equations could be applied. In order to facilitate the calculation of the net mass flux Bq in (2.14), however, we adopt here the averaging, not over the cross-section of the 'main flow' in the throat, but, over its whole cross-section, including the boundary layer. Then the equation of continuity simply becomes

$$\frac{\partial \overline{\rho}}{\partial t} + \frac{\partial}{\partial z}(\overline{\rho w}) = 0, \tag{2.15}$$

where z is the axial coordinate along the throat as shown in figure 2 with its origin at the orifice 1; $\overline{\rho}$ and $\overline{\rho w}$ denote, respectively, the mean density and mass flux density averaged over the whole cross-section. Because of the non-slip conditions on the throat wall, the right-hand side vanishes, unlike (2.1).

The equation of motion in the axial direction should now be modified to include the wall friction:

$$\frac{\partial}{\partial t}(\overline{\rho w}) + \frac{\partial}{\partial z}(\overline{\rho w^2}) = -\frac{\partial \overline{p}}{\partial z} + (\tfrac{4}{3}\mu + \mu_v)\frac{\partial^2 \overline{w}}{\partial z^2} - \frac{\sigma}{B}, \tag{2.16}$$

where $\overline{\rho w^2}$, $\overline{p}$, and $\overline{w}$ denote, respectively, the mean momentum flux density, pressure, and axial velocity averaged over the whole cross-section, while σ stands for the wall friction per unit axial length of the throat.

Here it might be appropriate to mention the difference in averaging, i.e. over the cross-section of the 'main flow' and the whole cross-section. A difference is clearly seen on comparing (2.15) and (2.16) with (2.1) and (2.2). According to the definition of averaging, each averaged quantity differs slightly by an amount proportional to the first order of deviations. If this difference is carefully taken into account, the resultant equation by one definition can be converted to the other as far as the present approximation is concerned.

In order to specify the mass flux from the resonator into the tunnel, we examine the response of the resonator. From the assumption that the throat is far shorter than a wavelength of the acoustic waves, compressibility of the gas in the throat may be neglected. To see this, the magnitude of the mass flux density $\overline{\rho w}$ is estimated from (2.16) to be $\Delta p/\omega L$ where the mass flux is brought about by the pressure difference Δp between both ends of the throat. Thus it is found that

$$|\partial \overline{\rho}/\partial t/\partial(\overline{\rho w})/\partial z| \sim (\omega L)^2 \Delta\rho/\Delta p \sim (L/\Lambda)^2 \ll 1,$$

where $\Delta\rho$ is a variation in the density due to Δp and a_0/ω is a characteristic wavelength Λ by using $\Delta p/\Delta\rho \approx a_0^2$. For $L \ll \Lambda$, the gas in the throat may be regarded as being incompressible. With the neglect of the smallness factor $(L/\Lambda)^2$, $\overline{\rho w}$ may be set equal to constant along the throat as

$$\overline{\rho w} = q(t). \tag{2.17}$$

Using (2.17) in (2.16) and neglecting the quadratic momentum flux density, we have, on integrating (2.16) with respect to z from one orifice 1 to the other orifice 2:

$$L\frac{\partial q}{\partial t} = -p_2 + p_1 - Fr, \quad \text{with } Fr = \frac{L\sigma}{B}, \tag{2.18}$$

where p_1 and p_2 denote the pressure at the orifices 1 and 2, respectively. Here the viscous term in (2.16) vanishes by virtue of the first-order relation of (2.17), i.e. $q \approx \rho_0 \bar{w}$ and the wall friction is uniform along the throat.

To evaluate the total friction Fr, the boundary layer must be examined. Unlike the case in the tunnel, we have only to take account of the boundary layer for the velocity because of the incompressible approximation. The axial velocity is similarly decomposed into a sum of $\bar{w}(t)$ and $w'(t, y)$ where y designates the coordinate directed inward normal to the throat wall. Then w' obeys the same heat equation (2.9a) as u' with n replaced by y. By solving this equation, σ is given by $\mu \partial w'/\partial y$ at $y = 0$ multiplied by the perimeter of the cross-section $2B/r$, r being the hydraulic radius of the throat. Although the heat equation is easily solved, we demonstrate the easiest way to do so. Since $\partial w'/\partial y$ is desired, the heat equation for w' is factorized, if the half-order derivative defined by (2.13) is employed, as

$$\frac{\partial w'}{\partial t} - \nu \frac{\partial^2 w'}{\partial y^2} = \left(\frac{\partial^{\frac{1}{2}}}{\partial t^{\frac{1}{2}}} - \nu^{\frac{1}{2}} \frac{\partial}{\partial y}\right)\left(\frac{\partial^{\frac{1}{2}}}{\partial t^{\frac{1}{2}}} + \nu^{\frac{1}{2}} \frac{\partial}{\partial y}\right) w' = 0. \tag{2.19}$$

Because the positive domain of y is concerned here, the second factor should be taken, in view of the matching conditions, $w' \to 0$ as $y \to \infty$. The choice is easily verified by examining the dispersion relation of each factor. Assuming w' proportional to $\exp(\mathrm{i}\omega t + \kappa y)$, it follows from the first factor, for example, that $\kappa = (\mathrm{i}\omega/\nu)^{\frac{1}{2}} = (\omega/2\nu)^{\frac{1}{2}}(1+\mathrm{i})$ where the half-order derivative of $\exp(\mathrm{i}\omega t)$ is simply given by $(\mathrm{i}\omega)^{\frac{1}{2}} \exp(\mathrm{i}\omega t) = (\frac{1}{2}\omega)^{\frac{1}{2}}(1+\mathrm{i}) \exp(\mathrm{i}\omega t)$. Thus we immediately derive

$$\mu \left.\frac{\partial w'}{\partial y}\right|_{y=0} = -\mu \nu^{-\frac{1}{2}} \left.\frac{\partial^{\frac{1}{2}} w'}{\partial t^{\frac{1}{2}}}\right|_{y=0} = \rho_0 \nu^{\frac{1}{2}} \frac{\partial^{\frac{1}{2}} \bar{w}}{\partial t^{\frac{1}{2}}}, \tag{2.20}$$

where use is made of the non-slip condition $w' = -\bar{w}$ at $y = 0$. Using (2.20), the total friction Fr is now expressed in term of q:

$$Fr = \frac{L\sigma}{B} = \frac{L}{B}\left(\frac{2B}{r} \mu \left.\frac{\partial w'}{\partial y}\right|_{y=0}\right) = \frac{2L}{r} \nu^{\frac{1}{2}} \frac{\partial^{\frac{1}{2}}}{\partial t^{\frac{1}{2}}} (\rho_0 \bar{w}). \tag{2.21}$$

Let us now derive an equation describing the response of the resonator. Assuming that the density change in the cavity occurs adiabatically, and that the pressure p_c may be set equal to p_2 at the orifice 2, the first-order relation of (2.14) is given by

$$q \approx \rho_0 \bar{w} = \frac{V}{B} \frac{\partial \rho_c}{\partial t} = \frac{V}{B a_0^2} \frac{\partial p_c}{\partial t} = \frac{V}{B a_0^2} \frac{\partial p_2'}{\partial t}, \tag{2.22}$$

where $\mathrm{d}p_c/\mathrm{d}\rho_c = a^2$ and $p_2' = p_2 - p_0$. Elimination of q in (2.18) by (2.22) and use of (2.21) lead to

$$\frac{\partial^2 p_2'}{\partial t^2} + \frac{2\nu^{\frac{1}{2}}}{r} \frac{\partial^{\frac{3}{2}} p_2'}{\partial t^{\frac{3}{2}}} + \omega_0^2 p_2' = \omega_0^2 p_1', \tag{2.23}$$

with $p_1' = p_1 - p_0$ where $\omega_0^2 (= Ba_0^2/LV)$ is the natural angular frequency of the resonator. Here p_1', the gauge pressure at the orifice 1 is assumed to be equal to that

pressure $p'(=p-p_0)$ in the main flow of the tunnel. Consistent with the variables used in (2.8), p_1' is related to the variation of a through

$$\frac{p_1'}{p_0}=\frac{p'}{p_0}=\frac{2\gamma}{\gamma-1}\left(\frac{a-a_0}{a_0}\right). \tag{2.24}$$

To conclude this subsection, we make the following remarks. A resonance frequency of the resonator to an external excitation is different, in practice, from the natural frequency ω_0 given above, even if the friction at the throat wall is taken into account. This results from the difficult problem known as the end correction of the throat. For a long throat which opens at both ends in a form of flanged termination, it is known from the inviscid and linear theory that the correction added at each end is given by $0.82r$ for a circular cross-section with $L \gg r$ (King 1936; Pierce 1981). However, since this result is derived for an orifice into semi-infinite space, it is an open question to what degree it could be applied to the present case. As for the end correction, we refer to the recent work by Monkewitz & Nguyen-Vo (1985) who refined the theory, though for geometrically different resonators, by the matched-asymptotic expansion method in terms of the ratio of a radius of a throat to a characteristic wavelength. With suitable corrections not only for the length of the throat but also for the size of the cavity, it is verified that the resonance frequency is still given by ω_0 in the elementary theory as the lowest approximation.

This result is derived by the inviscid and linear theory. In reality, a similar correction should also be introduced for the friction. Zinn (1970) added to L the viscous end corrections $2r$ found experimentally by Ingard (1953). The friction allowed by Zinn is insufficient because it takes account only of the so-called resistance (real) part of (2.21) for $\bar{w}$ in the form of a harmonic oscillation $\exp(i\omega t)$ and the reactance (imaginary) part is ignored. While this correction is applied to the linear friction, nonlinear friction must be taken into account as the pressure disturbances in the tunnel become large. Then the resistance of the resonators will be enhanced because the kinetic energy of the jet formed on leaving an orifice is transformed into turbulence. In the Appendix, the nonlinear theory for the response of the resonator is developed, by which we can find a condition to justify the linear approximation of the response of the resonator.

2.3. *Spatial evolution equation*

We are now in a position to complete (2.8) by specifying the mass flux ρv_n due to the boundary layer and the resonators. For the resonators almost continuously distributed with equal axial narrow spacing d, let the number density be $N(=1/d)$. Then the mass flux per unit axial length can be given as

$$\frac{1}{A}\oint \rho v_n \,\mathrm{d}s \approx \frac{1}{A}\left[\left(\frac{2A}{R}-NB\right)\rho_0 v_b - NBq\right], \tag{2.25}$$

where R is the hydraulic radius of the pipe and NB accounts for the total cross-sectional area of the orifices per unit axial length. Note that A in (2.25) may be replaced by the area of the whole geometrical cross-section of the tunnel because the difference from that of the main flow yields the higher-order correction. Upon substituting (2.12) and (2.22) into (2.25), (2.8) is written as

$$\left[\frac{\partial}{\partial t}+(u\pm a)\frac{\partial}{\partial x}\right]\left(u\pm\frac{2}{\gamma-1}a\right)=\pm\frac{2Ca_0\nu^{\frac{1}{2}}}{R^*}\frac{\partial^{-\frac{1}{2}}}{\partial t^{-\frac{1}{2}}}\left(\frac{\partial u}{\partial x}\right)\mp\frac{V}{\rho_0 a_0 A d}\frac{\partial p_2'}{\partial t}+\nu_d\frac{\partial^2 u}{\partial x^2}, \tag{2.26}$$

with the signs vertically ordered, where $1/R^*$ is defined as $(1-NRB/2A)/R$ with $B/A = (r/R)^2$. Equation (2.26), coupled through the pressure in the cavity p_2' with (2.23) and (2.24) describes the bi-directional propagation of nonlinear acoustic waves in a long tunnel with the array of Helmholtz resonators. For unidirectional propagation in the positive axial direction, they can be simplified further. Since the members on the right-hand side of (2.26) are small, $u \pm 2a/(\gamma-1)$ may be set equal to constants, at the lowest approximation, known as Riemann invariants, along each characteristic defined by $\mathrm{d}x/\mathrm{d}t = u \pm a$ (the signs vertically ordered). To pursue a far-field propagation in the positive direction along $\mathrm{d}x/\mathrm{d}t = u+a$, we take account of those small corrections, whereas we use the lowest approximation $u/a_0 = [2/(\gamma-1)](a-a_0)/a_0$ along $\mathrm{d}x/\mathrm{d}t = u-a$ for the simple wave region. Hence (2.26) is simplified as

$$\frac{\partial u}{\partial t} + (a_0 + \tfrac{1}{2}(\gamma+1)u)\frac{\partial u}{\partial x} = \frac{Ca_0\nu^{\frac{1}{2}}}{R^*}\frac{\partial^{-\frac{1}{2}}}{\partial t^{-\frac{1}{2}}}\left(\frac{\partial u}{\partial x}\right) - \frac{V}{2\rho_0 a_0 A d}\frac{\partial p_2'}{\partial t} + \tfrac{1}{2}\nu_{\mathrm{d}}\frac{\partial^2 u}{\partial x^2}. \tag{2.27}$$

Here we introduce the non-dimensional retarded time $\theta[=\omega(t-x/a_0)]$ measured in a frame moving with the linear sound speed and the far-field space variable X $(=\epsilon\omega x/a_0)$, ω being a characteristic angular frequency. In addition, we normalize $[\frac{1}{2}(\gamma+1)]u/a_0$ and $[(\gamma+1)/2\gamma]p_2'/p_0$ by ϵf and ϵg, respectively, where f and g are of order unity and the factor $\frac{1}{2}(\gamma+1)$ is introduced for convenience. Since $p'/p_0 = \gamma u/a_0$ in the present approximation. ϵf measures also the pressure $[(\gamma+1)/2\gamma]p'/p_0$ in the tunnel. From (2.27) and (2.23), it follows that

$$\frac{\partial f}{\partial X} - f\frac{\partial f}{\partial \theta} = -\delta_R\frac{\partial^{\frac{1}{2}} f}{\partial \theta^{\frac{1}{2}}} + \beta\frac{\partial^2 f}{\partial \theta^2} - \kappa\frac{\partial g}{\partial \theta}, \tag{2.28}$$

$$\frac{\partial^2 g}{\partial \theta^2} + \delta_r\frac{\partial^{\frac{3}{2}} g}{\partial \theta^{\frac{3}{2}}} + \Omega g = \Omega f, \tag{2.29}$$

where the coefficients δ_R, β, K, δ_r and Ω are defined as

$$\left.\begin{aligned} \delta_R = C\frac{(\nu/\omega)^{\frac{1}{2}}}{\epsilon R^*}, \quad \beta = \frac{\nu_{\mathrm{d}}\omega}{2\epsilon a_0^2}, \quad K = \frac{V}{2\epsilon A d}, \\ \delta_r = \frac{2(\nu/\omega)^{\frac{1}{2}}}{r}, \quad \Omega = \left(\frac{\omega_0}{\omega}\right)^2. \end{aligned}\right\} \tag{2.30}$$

Here $(\nu/\omega)^{\frac{1}{2}}$ gives the thickness of the boundary layer so δ_R and δ_r measure the ratios of the boundary-layer thickness to the radius of the tunnel and that of the throat, respectively. The effect of diffusivity of sound is represented by β. Given a frequency ω and a magnitude of nonlinearity ϵ, δ_R and β take definite values for a fixed geometry of the tunnel. The effect of the array of resonators is controlled by the 'coupling parameter' K and the 'tuning parameter' Ω. A suitable design of the array is thus reduced to a choice of K and Ω.

By taking a plausible example, let us evaluate these coefficients. For an air at 15 °C, $a_0 = 340$ m/s, $\gamma = 1.40$, $Pr = 0.72$ and $\nu = 1.45\times10^{-5}$ m^2/s. Let the diameter of the tunnel be 10 m (i.e. $R = 5$ m and $A = 25\pi$ m^2), and let the cavity be a sphere of diameter 4 m (i.e. $V = \frac{32}{3}\pi$ m^3) with the circular throat of diameter 1 m (i.e. $r = 0.5$ m and $B = \frac{1}{4}\pi$ m^2) and of length $L = 3$ m. For this geometry of the resonator, the natural frequency ω_0 is 4.8 Hz. If we let a characteristic frequency of the acoustic waves ω be 10π rad/s (5 Hz), we have $\delta_R = 2.0\times10^{-4}/\epsilon$, $\beta = 4.9\times10^{-9}/\epsilon$, $\delta_r = 2.7\times10^{-3}$ and $K = 2.1\times10^{-2}/\epsilon$ for $d = 10$ m $(N = 0.1/\mathrm{m})$ where $C = 1+(\gamma-1)/Pr^{\frac{1}{2}} = 1.47$ and μ_{v}/μ in ν_{d} is set equal to 0.60 (Pierce 1981). According

to these data, β/δ_R is extremely small (of order 10^{-5}) so that it could be ignored in (2.28). If ϵ is taken to be moderately small, for example, 2×10^{-3} (the magnitude of the pressure disturbances $p'/p_0=[2\gamma/(\gamma+1)]\epsilon=2.33\times10^{-3}$, i.e. 141 dB in the sound pressure level), it is found that δ_R and K are of order of 0.1 and 10, respectively. Although δ_r for the friction at the throat wall is relatively small, it can be increased by effectively making the radius r small, for example, by subdividing the throat axially into a bundle of throats.

Because we can choose the parameters K and Ω, we look at (2.28) and (2.29) in the extreme cases where K or Ω is taken to be very small or very large. In the trivial case with $K\ll1$, (2.28) describes simply the evolution in a tunnel without the array of resonators. In the opposite case with $K\gg1$, the effect of resonators dominates over the nonlinearity and the effect of boundary layer so that the evolution of f, $\partial f/\partial X$, is given almost by $-K\partial g/\partial\theta$. With this relation substituted into (2.29), we have the linear dispersive wave equation for f

$$\frac{\partial f}{\partial X}+K\frac{\partial f}{\partial\theta}+\frac{1}{\Omega}\frac{\partial^3 f}{\partial\theta^2\partial X}+\frac{\delta_r}{\Omega}\frac{\partial^{\frac{3}{2}}}{\partial\theta^{\frac{3}{2}}}\left(\frac{\partial f}{\partial X}\right)=0. \tag{2.31}$$

However, it should be borne in mind that an extremely large value of K, i.e. V/Ad, invalidates the basic assumption of small reflection by each resonator connected discretely in practice.

Next we examine the extreme cases for Ω. For $\Omega\ll1$, Ωg in (2.29) may be dropped in the response of f. On eliminating g in (2.28) and (2.29), it then follows that

$$\left(\frac{\partial}{\partial\theta}+\delta_r\frac{\partial^{\frac{1}{2}}}{\partial\theta^{\frac{1}{2}}}\right)\left(\frac{\partial f}{\partial X}-f\frac{\partial f}{\partial\theta}+\delta_R\frac{\partial^{\frac{1}{2}}f}{\partial\theta^{\frac{1}{2}}}-\beta\frac{\partial^2 f}{\partial\theta^2}\right)=-K\Omega f. \tag{2.32}$$

As $K\Omega$ is negligibly small, the factor in the second parentheses on the left-hand side must vanish so that the evolution of f is tantamount to that in the tunnel without the resonators. In this case, it is already found that if the term with β is ignored, the evolution equation resembles a hyperbolic type of wave equation so that shock waves generally emerge (Sugimoto 1991). Even if $K\Omega$ becomes of $O(1)$, (2.32) still preserves such properties because the additional term on the right-hand side is lower order (zeroth) in differentiation than that of the nonlinear term. Therefore, it is unavoidable that shock waves will eventually appear in this case.

For $\Omega\gg1$, on the other hand, (2.29) may be approximated as

$$g=f-\frac{1}{\Omega}\left(\frac{\partial^2 g}{\partial\theta^2}+\delta_r\frac{\partial^{\frac{3}{2}}g}{\partial\theta^{\frac{3}{2}}}\right)=f-\frac{1}{\Omega}\left(\frac{\partial^2 f}{\partial\theta^2}+\delta_r\frac{\partial^{\frac{3}{2}}f}{\partial\theta^{\frac{3}{2}}}\right)+O\left(\frac{1}{\Omega^2}\right). \tag{2.33}$$

Neglecting the order of Ω^{-2}, we have from (2.28)

$$\frac{\partial f}{\partial X}+K\frac{\partial f}{\partial\theta}-f\frac{\partial f}{\partial\theta}=-\delta_R\frac{\partial^{\frac{1}{2}}f}{\partial\theta^{\frac{1}{2}}}+\beta\frac{\partial^2 f}{\partial\theta^2}+\frac{K}{\Omega}\left(\frac{\partial^3 f}{\partial\theta^3}+\delta_r\frac{\partial^{\frac{5}{2}}f}{\partial\theta^{\frac{5}{2}}}\right). \tag{2.34}$$

This equation is the Korteweg–de Vries–Burgers equation which takes account of the hereditary effect due to the boundary layer. Furthermore, if both the diffusivity and hereditary effects are negligibly small, (2.34) is reduced to the well-known Korteweg–de Vries equation (see, e.g. Whitham 1974; Drazin & Johnson 1989):

$$\frac{\partial f}{\partial X}+K\frac{\partial f}{\partial\theta}-f\frac{\partial f}{\partial\theta}=\frac{K}{\Omega}\frac{\partial^3 f}{\partial\theta^3}. \tag{2.35}$$

The third-order derivative can compete with the nonlinear steepening to allow propagation of a smooth solidary wave, now well-known as a soliton. In this special case, a shock wave can no longer be propagated.

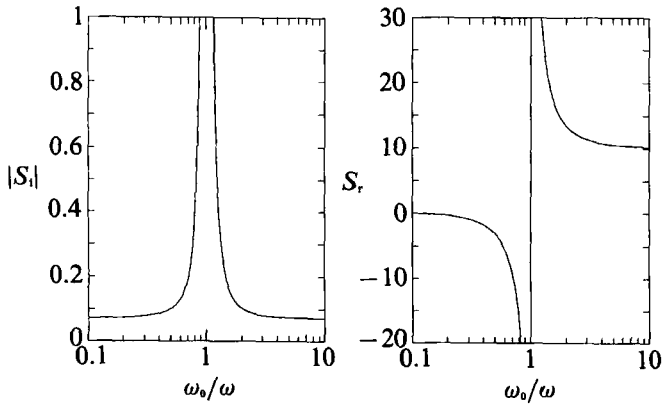

FIGURE 3. Dispersion relation for the linear acoustic waves in the tunnel with an array of Helmholtz resonators where the inverse of the phase velocity S (i.e. slowness) is given as a function of ω_0 normalized by ω: (*a*) and (*b*) show, respectively, its imaginary part $|S_i|$ and its real part S_r versus ω_0/ω for $\delta_R = 0.1$, $\delta_r = 0.01$ and $K = 10$.

2.4. *Dispersion relation*

Before considering the full problems, let us examine the linear dispersion relation to see how the resonators contribute to the damping of the acoustic waves. Assuming that f and g are proportional to $\exp[\mathrm{i}(\theta - SX)]$ where S (which should not be confused with the entropy used before) is constant, we have

$$S = \mathrm{i}^{-\frac{1}{2}}\delta_R - \mathrm{i}\beta + \frac{K\Omega}{\Omega - 1 + \mathrm{i}^{\frac{3}{2}}\delta_r}, \tag{2.36}$$

where, remember, that the frequency ω is involved not only in Ω but also in δ_R, β, and δ_r and that S corresponds physically to an inverse of a phase velocity called a slowness. The imaginary part of S ($\equiv S_r + iS_i$) gives the spatial decay with respect to X. From (2.36), it follows that

$$S_i = -\frac{1}{\sqrt{2}}\delta_R - \beta - \frac{1}{\sqrt{2}}\frac{\delta_r K\Omega}{(\Omega - 1 - \delta_r/\sqrt{2})^2 + \frac{1}{2}\delta_r^2}. \tag{2.37}$$

While the first and second terms represent the inherent decay of acoustic waves owing to the wall friction and the diffusivity of sound itself, respectively, the last term represents the very enhancement of decay by the array of Helmholtz resonators. If S_i is regarded as a function of ω_0 with ω fixed, $|S_i|$ has a maximum

$$\max|S_i| = \frac{1}{\sqrt{2}}\delta_R + \beta + \frac{\delta_r K}{8^{\frac{1}{2}}(\Omega - 1 - \delta_r/\sqrt{2})} = \frac{1}{\sqrt{2}}\delta_R + \beta + \frac{\sqrt{2}}{\delta_r}(1 + \sqrt{2}\delta_r + \ldots)K$$

at

$$\Omega = \Omega_0 = (1 + \sqrt{2}\delta_r + \delta_r^2)^{\frac{1}{2}} = 1 + \delta_r/\sqrt{2} + \tfrac{1}{4}\delta_r^2 + \ldots. \tag{2.38}$$

Since β is far smaller than δ_R, the effect due to the diffusivity is secondary behind the wall friction. Figure 3 (*a*) depicts the damping rate $|S_i|$ as a function of ω_0 normalized by ω for the values of parameters $\delta_R = 0.1$, $\delta_r = 0.01$ and $K = 10$ where β is ignored. Hence, if the resonators are appropriately designed, they will enhance significantly the decay of acoustic waves in the tunnel. Here it is noted that this decay characteristic is not necessarily valid in the case of nonlinear acoustic waves, as we shall see later.

In addition to the decay, the resonators can also give rise to the dispersion. From (2.36), in fact, the real part of S gives

$$S_r = \frac{1}{\sqrt{2}}\delta_R + \frac{K\Omega(\Omega - 1 - \delta_r/\sqrt{2})}{(\Omega - 1 - \delta_r/\sqrt{2})^2 + \frac{1}{2}\delta_r^2}. \tag{2.39}$$

Figure 3(*b*) depicts S_r versus ω_0/ω. In the limit as $\omega_0/\omega \to 0$, S_r approaches $\delta_R/\sqrt{2}$ for a tunnel without resonators. It is found that the boundary-layer effect gives rise not only to the decay but also to the delay of propagation. In the other limit, as $\omega_0/\omega \to \infty$, the array of resonators contributes to the further delay and S_r approaches $\delta_R/\sqrt{2}+K$.

3. Evolution of nonlinear acoustic waves

On the basis of (2.28) and (2.29), we examine an effect of the array of Helmholtz resonators on propagation of nonlinear acoustic waves. The effect due to the diffusivity of sound is sufficiently small that the term with β in (2.28) may be neglected. For a tunnel without an array of resonators (called a simple tunnel hereinafter), the diffusivity of sound has a primary role only locally in a thin shock layer, outside of which it always remains secondary behind the global effect due to the wall friction (Sugimoto 1991). In view of this result, the second-order derivative of f in (2.28) is neglected in the following because interest is focused on the global effects of the resonators and the boundary layer.

3.1. *Relations for the discontinuity*

In the simple tunnel, it is already known that the wall friction fails to compete with the nonlinear steepening, unlike the diffusivity of sound, which allows the emergence of a discontinuity, i.e. shock wave. First, therefore, we examine whether or not the propagation of a discontinuity is possible even when the resonators are connected.

Suppose a discontinuity in f and g be located at $\theta = \tau(X)$. Introducing a new variable η defined by $\eta = \theta - \tau(X)$ instead of θ, (2.28) and (2.29) are written in terms of η and X as follows:

$$\frac{\partial f}{\partial X} - \dot{\tau}\frac{\partial f}{\partial \eta} - \frac{\partial}{\partial \eta}(\tfrac{1}{2}f^2) = -\delta_R \frac{\partial^{\frac{1}{2}} f}{\partial \eta^{\frac{1}{2}}} - K\frac{\partial g}{\partial \eta}, \tag{3.1}$$

$$\frac{\partial^2 g}{\partial \eta^2} + \delta_r \frac{\partial^{\frac{3}{2}} g}{\partial \eta^{\frac{3}{2}}} + \Omega g = \Omega f, \tag{3.2}$$

where the dot denotes differentiation with respect to X. Let continuous solutions $f = F(\eta, X)$ and $g = G(\eta, X)$ to (3.1) and (3.2) be prevalent in the region $-\infty < \eta < 0$. Assume that F and G be appropriately smooth enough around $\eta = 0$ to be continued beyond it as

$$\left.\begin{aligned} F(\eta, X) &= F_0 + F_2\eta + F_4\eta^2 + \ldots + F_n\eta^{\frac{1}{2}n} + \ldots, \\ G(\eta, X) &= G_0 + G_2\eta + G_4\eta^2 + \ldots + G_n\eta^{\frac{1}{2}n} + \ldots, \end{aligned}\right\} \tag{3.3}$$

where $|\eta| \ll 1$ and F_n and G_n $(n = 0, 2, 4, \ldots)$ are functions of X. The solutions including the discontinuity at $\eta = 0$ are assumed to be expressed locally as

$$\left.\begin{aligned} f &= F(\eta, X) + [V_0 + V_1|\eta|^{\frac{1}{2}} + \ldots + V_n|\eta|^{\frac{1}{2}n} + \ldots]\,h(\eta), \\ g &= G(\eta, X) + [W_0 + W_1|\eta|^{\frac{1}{2}} + \ldots + W_n|\eta|^{\frac{1}{2}n} + \ldots]\,h(\eta), \end{aligned}\right\} \tag{3.4}$$

where $h(\eta)$ denotes the unit step function; V_n and W_n $(n = 0, 1, 2, \ldots)$ are functions of X. As was already demonstrated by Sugimoto (1991), this half-power expansion of $|\eta|$ behind the discontinuity, i.e. $\eta > 0$, is suggested by the following formula of the fractional derivatives:

$$\frac{\mathrm{d}^q}{\mathrm{d}\eta^q}\frac{|\eta|^p h(\eta)}{\Gamma(p+1)} = \frac{|\eta|^{p-q} h(\eta)}{\Gamma(p+1-q)}, \tag{3.5}$$

where $p = \frac{1}{2}n$ $(n = 0, 1, 2, \ldots)$ and $q = \frac{1}{2}$ or $\frac{3}{2}$ in the present context; $\Gamma(p)$ denotes the Gamma function.

Although the discontinuity in g is expanded formally from W_0, it is found from (3.2) that W_n should vanish for $n = 0$ to $n = 3$. Substituting (3.4) into (3.1) and identifying $h(\eta)^2$ resulting from f^2 to be $h(\eta)$, we have from the coefficient of the delta function $\delta(\eta)[= \mathrm{d}h(\eta)/\mathrm{d}\eta]$:

$$\dot{\tau} = -(F_0 + \tfrac{1}{2}V_0). \tag{3.6}$$

Proceeding with the expansion in (3.1) successively, we derive from the coefficients of $|\eta|^{n/2-1}h(\eta)\,(n = 1, 2, 3, \ldots)$:

$$\left.\begin{aligned} &V_1 = \frac{4\delta_R}{\pi^{\frac{1}{2}}}, \quad V_2 = \frac{2}{V_0}\left[\dot{V}_0 + 2\delta_R^2\left(1 - \frac{4}{\pi}\right)\right] - 2F_2, \\ &V_n = \frac{4}{nV_0}\Big[\dot{V}_{n-2} - \tfrac{1}{2}n(F_2 V_{n-2} + F_4 V_{n-4} + \ldots + F_n V_0) \\ &\qquad - \tfrac{1}{4}n(V_1 V_{n-1} + \ldots + V_{n-1} V_1) + \delta_R \frac{\Gamma[\frac{1}{2}(n+1)]}{\Gamma(\frac{1}{2}n)} V_{n-1} + \tfrac{1}{2}Kn W_n\Big] \quad (n = 3, 4, 5, \ldots), \end{aligned}\right\} \tag{3.7}$$

where F_n vanish for odd n. From (3.2), similarly, we have

$$W_n = -\frac{4}{n(n-2)}\left[\Omega(W_{n-4} - V_{n-4}) + \delta_r \frac{\Gamma[\frac{1}{2}(n+1)]}{\Gamma(\frac{1}{2}n-1)} W_{n-1}\right] \quad (n = 4, 5, 6, \ldots), \tag{3.8}$$

where $W_0 = W_1 = W_2 = W_3 = 0$. It is the inertia of the resonator that makes W_n vanish for $n = 0$ to $n = 3$. Therefore, the resonators respond to the discontinuity very slowly. Since (3.6) is free from K, it is found that the propagation of the discontinuity is unaffected by the resonators explicitly. It will be shown later, however, that they will suppress the emergence of the discontinuity indirectly by dispersing the acoustic waves.

3.2. *Steady discontinuous solution*

As a simple example of the preceding subsection, let us examine a steady and discontinuous solution propagating with a constant velocity into the equilibrium state ahead $F = G = 0$. Setting $\dot{\tau}$ to be a constant $1/\lambda$ (> 0) where λ is a velocity, we assume that f and g depend only on $\zeta(= \theta - X/\lambda)$. Even under the 'steady assumption', it is still difficult to solve (3.1) and (3.2) analytically. Thus, numerical solutions are sought by making use of the asymptotic relations around the discontinuity.

In choosing values of parameters, the following points are remarked. If the nonlinear parameter ϵ is measured by a magnitude of discontinuity, V_0 is set equal to unity. Because no characteristic timescale is involved in this problem, ω may be chosen to be ω_0 so that Ω may be set equal to unity. Then δ_R and δ_r take the definite

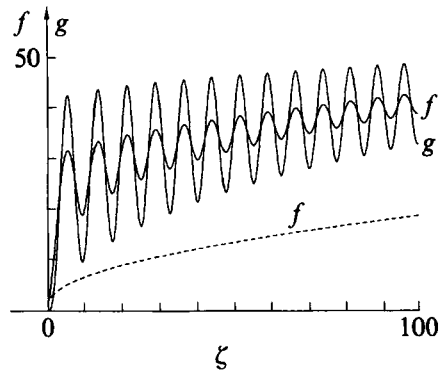

FIGURE 4. Profiles of steady discontinuous solutions of f and g for $\delta_R = 1$, $\delta_r = 0.01$, $K = 10$ and $\Omega = 1$. For reference, the profile of f in a case without resonators is shown in the broken lines for the same value of δ_R.

values δ_{R0} and δ_{r0}, respectively. Alternatively if ω be chosen so that δ_R may be normalized, then δ_r and Ω should read, respectively, δ_{r0}/δ_{R0} and δ_{R0}^{-4}.

Figure 4 shows the discontinuous solutions of f and g with $V_0 = 1$ versus $\zeta = \theta + \frac{1}{2}X$ for the parameters $\delta_R = 1$, $\delta_r = 0.01$, $K = 10$ and $\Omega = 1$. For reference, the profile of f in the simple tunnel is shown by the broken lines for $\delta_R = 1$ (Keller 1981; Sugimoto 1989). It is seen that the resonators make the profiles of f and g oscillatory, owing to the dispersion. In contrast, the dispersion due to the wall friction does not yield any oscillatory profile.

As ζ becomes large, it is confirmed numerically that f and g increase indefinitely, while the oscillation gradually decays out. The asymptotic analysis as $\zeta \to \infty$ indicates that

$$f = g = \delta_R(\pi\zeta)^{\frac{1}{2}} + \frac{\pi}{2(\pi-2)}(V_0+2K) + \frac{\pi^{\frac{1}{2}}(\pi-4)(V_0+2K)^2}{8\delta_R(\pi-2)^2\log 4}\zeta^{-\frac{1}{2}}\log\zeta + O(\zeta^{-\frac{1}{2}}) \quad \text{as } \zeta\to\infty, \tag{3.9}$$

where f is equal to g within the first three terms. In this limit of large ζ, the effect of resonators is secondary.

Even if a value of K is changed, oscillatory profiles of f and g are commonly observed. As K becomes smaller than 10, the oscillation tends to be small. For other choices of the parameter δ_R as well, the oscillatory profiles do appear and the damping of the oscillation is controlled by the value of δ_r. As δ_r becomes large, the oscillation rapidly decays out.

3.3. *Initial-value problems*

We now consider the initial-value problems for (2.28) and (2.29) in which the diffusivity of sound is ignored. To this end, it is convenient to express them in the 'characteristic form' as

$$\frac{\mathrm{d}f}{\mathrm{d}X} = -\delta_R\frac{\partial^{\frac{1}{2}}f}{\partial\theta^{\frac{1}{2}}} - K\frac{\partial g}{\partial\theta}, \tag{3.10}$$

with

$$\frac{\partial^2 g}{\partial\theta^2} + \delta_r\frac{\partial^{\frac{3}{2}}g}{\partial\theta^{\frac{3}{2}}} + \Omega g = \Omega f, \tag{3.11}$$

along the 'characteristics' defined by

$$\frac{\mathrm{d}\theta}{\mathrm{d}X} = -f. \tag{3.12}$$

An initial condition for f is prescribed on $X = 0$ as

$$f(\theta, X = 0) = f_0(\theta). \tag{3.13}$$

An initial condition for g should be given as a solution to (3.11) with $f = f_0$. It is remarked that although the condition (3.13) provides an initial value for (3.10), it corresponds physically to the boundary condition prescribed on $x = 0$ and (3.10) describes the spatial evolution. In the following, we consider three types of conditions for f_0; a unit step function, a Gaussian-shaped positive pulse and a pair of positive and negative pulses given by the derivative of the Gaussian-shaped pulse:

I. a step: $f_0 = h(\theta)$
II. a positive pulse: $f_0 = \exp(-\theta^2)$,
III. a pair of positive and negative pulses: $f_0 = -(2e)^{\frac{1}{2}}\theta \exp(-\theta^2)$,

where the maximum of f_0 is normalized to unity.

The initial-value problem is solved numerically by integrating (3.10) and (3.11) along (3.12). For a given f_0, (3.11) is first solved to derive $g = g_0$ at $X = 0$. This is to solve the integro-differential equation for g because of the three-half-order derivative of g. With g_0 thus obtained, $\partial g_0/\partial\theta$ is easily available so that the right-hand side of (3.10) can be evaluated together with the half-order derivative of f_0. This process is done numerically by discretizing θ (not necessarily equi-distantly). At each point of θ, (3.12) gives the slope of the characteristic, which is approximated by a straight line between $X = 0$ and $X = \Delta X \ll 1$. Along this line, (3.10) is replaced by the simplest forward difference so that a new value of f at $X = \Delta X$ is evaluated. Using f thus obtained, g is renewed by solving (3.11). Advancing this scheme by ΔX successively, the spatial evolutions of f and g are sought.

As soon as the multi-valuedness in f happens in the course of calculation, a discontinuity is fitted according to the so-called equal-area rule (Whitham 1974). For localized initial conditions, (3.10) stipulates that the total area under f is conserved with respect to X (Sugimoto 1991). Further evolution of the discontinuity is determined by the relations derived in §3.1. A position of the discontinuity is calculated by integrating (3.6), while its magnitude is determined by fitting locally the asymptotic solutions (3.4). Evolutions of f and g are not pursued over a sufficiently long distance of X until shock waves finally disappear because of the present concern on the possibility of the emergence of shock waves.

3.3.1. *Case I*: $f_0 = h(\theta)$

In contrast to the case of the steady but unbounded discontinuous solution, it is interesting to examine evolution from the unit step. Since the initial condition involves the discontinuity, its evolution must be taken into account from the outset by using the asymptotic relations. Figure 5 shows the spatial evolutions of f and g for $\delta_R = 1$, $\delta_\tau = 0.01$, $K = 10$ and $\Omega = 1$. To show the initial profile of g explicitly, the direction of the X-axis is taken reversed in figure 5(*b*). The dispersive character makes the profile of f undulatory, which is to be compared with the monotonically increasing one in the simple tunnel (Sugimoto 1990). The vicinity of the wavefront is seen to be segregated to form a triangular pulse. In the profile behind this pulse,

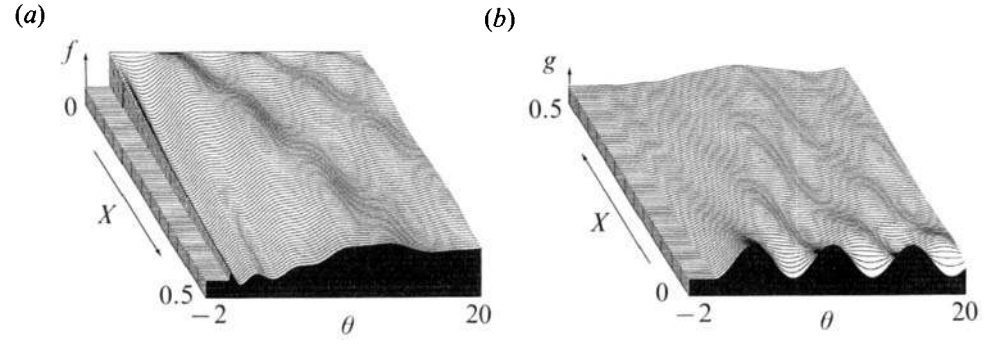

FIGURE 5. Spatial evolutions from a step for f up to $X = 0.5$ where (a) and (b) show the evolution of f and g, respectively for $\delta_R = 1$, $\delta_r = 0.01$, $K = 10$ and $\Omega = 1$ and the length of the vertical arrows measures unity of f and g.

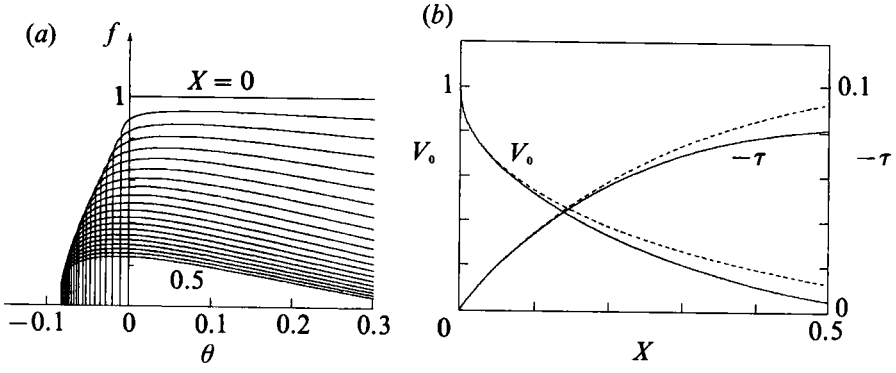

FIGURE 6. (a) Local profiles of f around the discontinuity up to $X = 0.5$ by steps in X of 0.025 for $\delta_R = 1$, $\delta_r = 0.01$, $K = 10$ and $\Omega = 1$; (b) spatial variations of the magnitude of the discontinuity $V_0(X)$ and its location $\tau(X)$ obtained from the evolution shown in (a), where the broken lines represent those in the simple tunnel with the same value of $\delta_R = 1$.

there is no indication of new emergence of discontinuities up to $X = 0.5$. Figure 6(a) shows the local profile of f around the discontinuity. As in the simple tunnel, the effect of the boundary layer makes the discontinuity round-edged. Figure 6(b) shows the spatial variations of the magnitude of the discontinuity $V_0(X)$ and its location $\tau(X)$ where the broken lines correspond to those in the simple tunnel for reference. It is confirmed that the resonators do not affect propagation of the discontinuity itself.

3.3.2. *Case II*: $f_0 = \exp(-\theta^2)$

Next we examine evolution from a positive pulse. It is already known that, in the simple tunnel, the shock wave appears at the leading edge for a value of δ_R smaller than about 0.5 (Sugimoto 1990, 1991). Thus, interest is focused on how the array of resonators affects emergence of shock waves by changing the coupling parameter K and the tuning parameter Ω. In view of the plausible values of the parameters, we fix δ_R and δ_r as 0.1 and 0.01, respectively, and examine evolutions for nine combinations of parameters for K and Ω among $K = 1$, 5 and 10 and $\Omega = 0.1$, 1 and 10. For comparison, the evolution in the simple tunnel is also shown in figure 7 for $\delta_R = 0.1$. It is seen that the initial pulse forms the shock wave at $X = 1.2550$ to evolve into the triangular pulse. In addition to rounding the shock wave, the effect of the boundary layer also produces the tail behind. At the final stage of calculation $X = 4$,

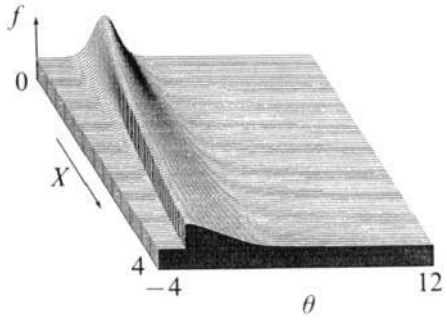

FIGURE 7. Spatial evolution from a positive pulse for f in the simple tunnel up to $X = 4$ where $\delta_R = 0.1$ and $K = 0$.

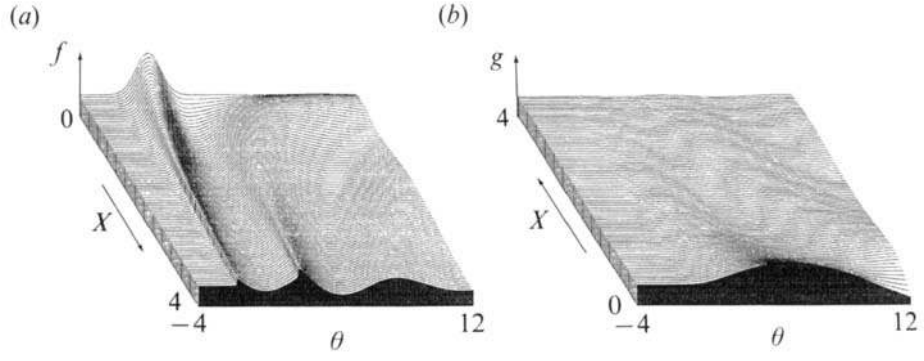

FIGURE 8. Spatial evolutions from a positive pulse for f up to $X = 4$ where (a) and (b) show the evolution of f and g, respectively, for $\delta_R = 0.1$, $\delta_r = 0.01$, $K = 10$ and $\Omega = 0.1$ and the length of the vertical arrows measures unity of f and g.

the shock wave is still of large magnitude. For reference, the unity of X corresponds physically to a distance 5.4 km for $\epsilon = 2 \times 10^{-3}$ and $\omega = 10\pi$ rad/s.

What will happen to this tunnel if the resonators are connected? In the following, the spatial evolutions are displayed by varying K first with Ω fixed. For $\Omega = 0.1$, the linear dispersion relation indicates no significant dissipation. The numerical calculations show, for all values of K chosen above, that the second shock wave is formed behind the leading one of the triangular pulse. Emergence of shock waves agrees with the anticipation by the approximate equation (2.32) for $\Omega \ll 1$ and $\beta = 0$. Figure 8 shows the typical evolutions of f and g for a relatively large value of $K = 10$. The leading shock wave emerges at $X = 1.8730$ while the second one emerges at $X = 3.8395$. It is seen that the magnitude of the second shock wave exceeds eventually that of the leading one. In this respect, the resonators make the situation worse, compared with the case for the simple tunnel.

For $\Omega = 1$, the significant dissipation is expected. For $K = 1$, however, the evolution is qualitatively similar to that shown in figure 8, although the oscillatory behaviour of g becomes rapid because of a larger value of Ω. As K is increased to $K = 5$ and 10, the initial pulse quickly decays out without any sign of shock waves. Figure 9 demonstrates the typical situation for $K = 10$. At $X = 4$, there remain only a few ripples.

For $\Omega = 10$, no shock wave emerges, even for $K = 1$, although the linear damping rate is much smaller than that in the case of $\Omega = 0.1$ and $K = 10$. Figure 10 shows the typical situation in which the initial pulse is delayed, i.e. propagated backward

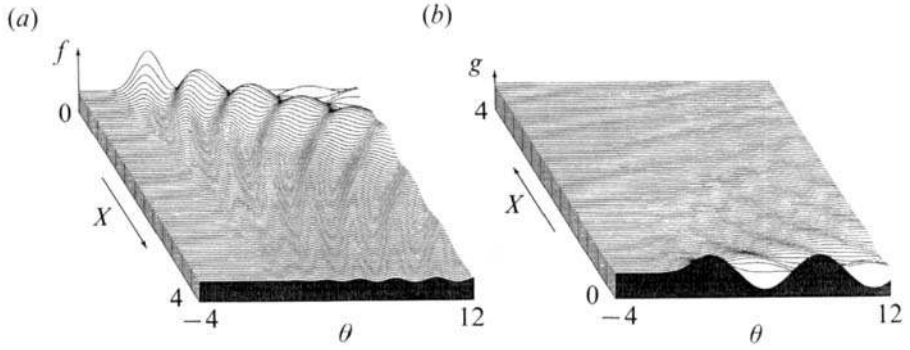

FIGURE 9. Spatial evolutions from a positive pulse for f up to $X = 4$ where (a) and (b) show the evolution of f and g, respectively for $\delta_R = 0.1$, $\delta_r = 0.01$, $K = 10$ and $\Omega = 1$ and the length of the vertical arrows measures unity of f and g.

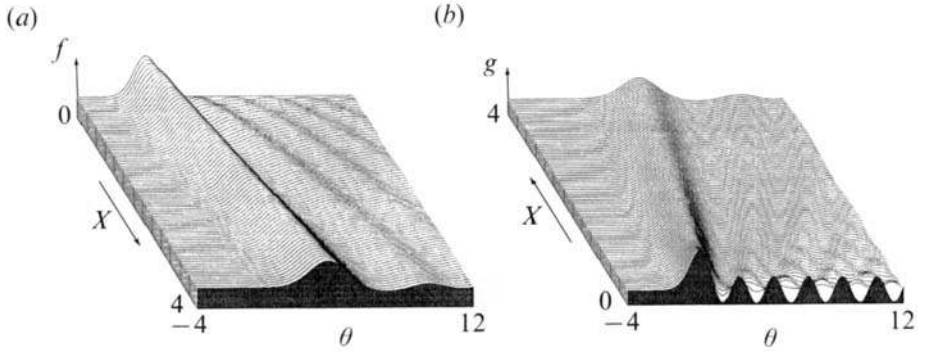

FIGURE 10. Spatial evolutions from a positive pulse for f up to $X = 4$ where (a) and (b) show the evolution of f and g, respectively, for $\delta_R = 0.1$, $\delta_r = 0.01$, $K = 1$ and $\Omega = 10$ and the length of the vertical arrows measures unity of f and g.

(rightward) without any sign of shock waves, at least up to $X = 4$. This result is understood by the approximate equation (2.34) for $\Omega \gg 1$ and $\beta = 0$. The term $K\partial f/\partial\theta$ represents the delay consistent with the dispersion relation (2.39) for $\Omega \gg 1$. The smooth profile is due to the dispersion, i.e. the third-order derivative, which can now compete with the nonlinear steepening to suppress the emergence of shock waves. As suggesting by (2.33), incidentally, it is seen that f and g tend to coincide with each other after the initial transient decays out.

3.3.3. *Case III*: $f_0 = -(2e)^{\frac{1}{2}}\theta\exp(-\theta^2)$

Finally we examine evolutions from a pair of positive and negative pulses. The spatial evolution in the simple tunnel is shown in figure 11. The pulses evolve into the so-called N-wave, though asymmetrically owing to the hereditary effect, and accompany the tail behind. The leading and trailing shock waves are formed at $X = 1.0265$ and $X = 1.0530$, respectively.

Let us examine the effect of resonators. For $\Omega = 0.1$, the leading and trailing shock waves appear for $K = 10$, as shown in figure 12, at $X = 1.3280$ and $X = 0.8535$, respectively, but the trailing one has no longer an expansion region, unlike in figure 11. Furthermore, it is remarked that the trailing shock wave grows greater than the leading one. For $\Omega = 1$, two shock waves are still formed for $K = 1$ just as shown in figure 13 at $X = 1.2960$ and $X = 0.8630$. In this case as well, the magnitude of the trailing shock wave exceeds that of the leading one. For $K = 5$, the leading shock

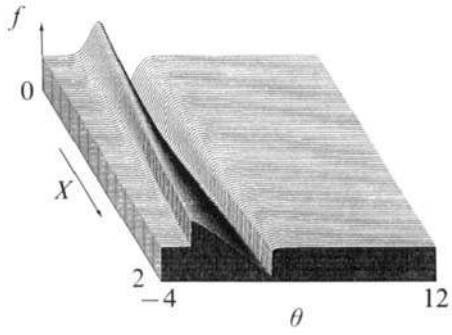

FIGURE 11. Spatial evolution from a pair of positive and negative pulses for f in the simple tunnel up to $X = 2$ where $\delta_R = 0.1$ and $K = 0$.

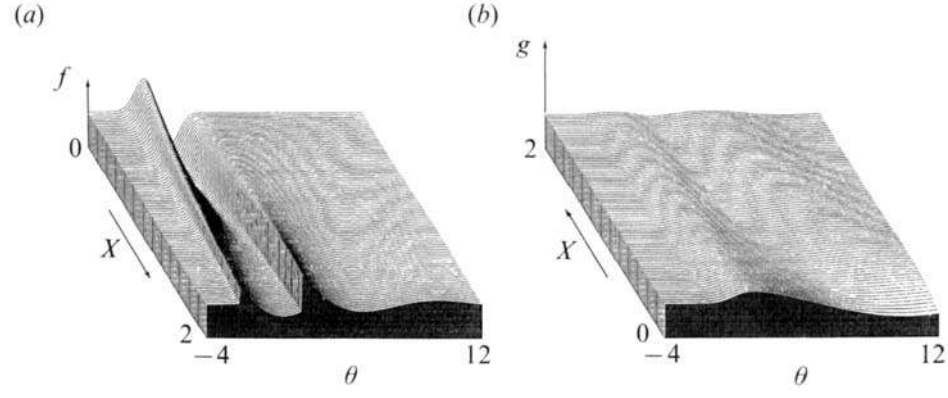

FIGURE 12. Spatial evolutions from a pair of positive and negative pulses for f up to $X = 2$ where (a) and (b) show the evolution of f and g, respectively for $\delta_R = 0.1$, $\delta_r = 0.01$, $K = 10$ and $\Omega = 0.1$ and the length of the vertical arrows measures unity f and g.

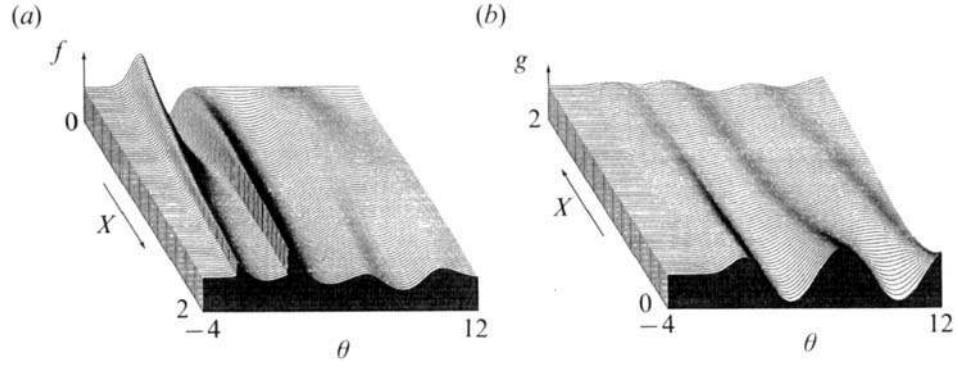

FIGURE 13. Spatial evolutions from a pair of positive and negative pulses for f up to $X = 2$ where (a) and (b) show the evolution of f and g, respectively for $\delta_R = 0.1$, $\delta_r = 0.01$, $K = 1$ and $\Omega = 1$ and the length of the vertical arrow measures unity.

wave is no longer formed so that only one shock wave appears. As K is increased further to 10, no shock wave emerges. Figure 14 shows the evolution in which the initial pulses develop into ripples. For $\Omega = 10$, finally, the evolution is qualitatively similar to case II. There appears to be no shock wave, even for $K = 1$, and the wave is propagated backward.

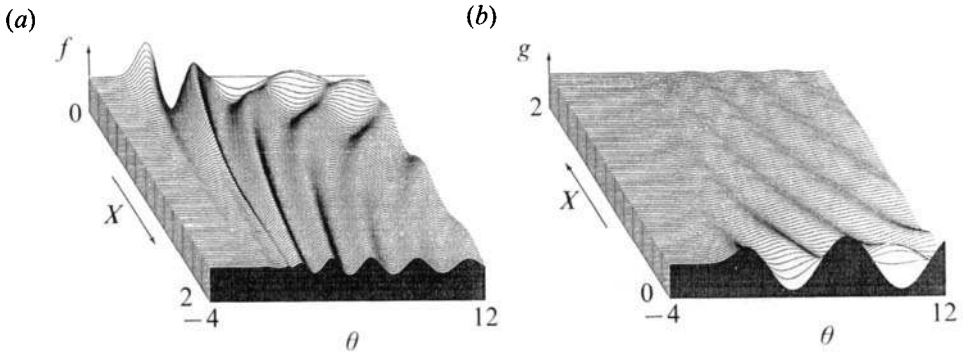

FIGURE 14. Spatial evolutions from a pair of positive and negative pulses for f up to $X = 2$ where (a) and (b) show the evolution of f and g, respectively, for $\delta_R = 0.1$, $\delta_r = 0.01$, $K = 10$ and $\Omega = 1$ and the length of the vertical arrows measures unity of f and g.

4. Results and concluding remarks

We have investigated the effect of the array of Helmholtz resonators on the propagation of nonlinear acoustic waves in a long tunnel. It is found that the resonators are very effective, if appropriately designed, in suppressing the shock waves which would emerge unless connected. It is emphasized that the resonators do not suppress shock waves once they are formed. They prevent the emergence of shock waves by introducing dispersion into acoustic waves in addition to damping.

In order to avoid shock waves for the case with $\epsilon = 2 \times 10^{-3}$, $\delta_R = 0.1$ and $\delta_r = 0.01$, as a typical example, the resonators are proved effective if the coupling parameter K is taken to be a large value such as 10, while the tuning parameter Ω is chosen greater than unity. Of course, greater values of K would give rise to higher damping, but there is a limitation of the present theory, i.e. $V/Ad \ll 1$. As Ω becomes greater than unity, it is found that even a smaller value of K is enough to delay or suppress the emergence of shock waves. In fact, if Ω is chosen to be 3 for $K = 1$, the emergence of shock waves is delayed significantly, as is shown in figure 15, to $X = 1.9415$ at $\theta = 5.2649$ in the evolution from a pair of pulses. A possible reason may be conjectured as follows. In the course of evolution, the nonlinearity gives rise to higher-frequency components than those involved in the initial profile, which lowers Ω substantially. Therefore, even if Ω is set, initially, to be 'tuned up' greater than unity, the nonlinearity lowers Ω effectively for the frequency containing the most energy to be located around $\Omega = 1$ so that higher damping would be expected rather than the case with $\Omega = 1$ initially.

In particular, it is a useful result that for a large value of Ω, there is no sign of emergence of shock waves even for a small value of K. In spite of the small linear damping rate as in the case with $\Omega \ll 1$, the smooth profiles are brought about by the dispersion due to the third-order derivative in (2.34). Furthermore, when the nonlinearity becomes relatively strong compared to the diffusivity and the hereditary effects, as the Korteweg–de Vries equation (2.35) stipulates, it becomes possible for an acoustic soliton to be propagated and its profile is given by

$$f = \alpha \operatorname{sech}^2[(\alpha\Omega/12K)^{\frac{1}{2}}(\theta - KX + \tfrac{1}{3}\alpha X - \theta_0)],$$

where α is a constant and positive amplitude and θ_0 is a phase constant (see, e.g.

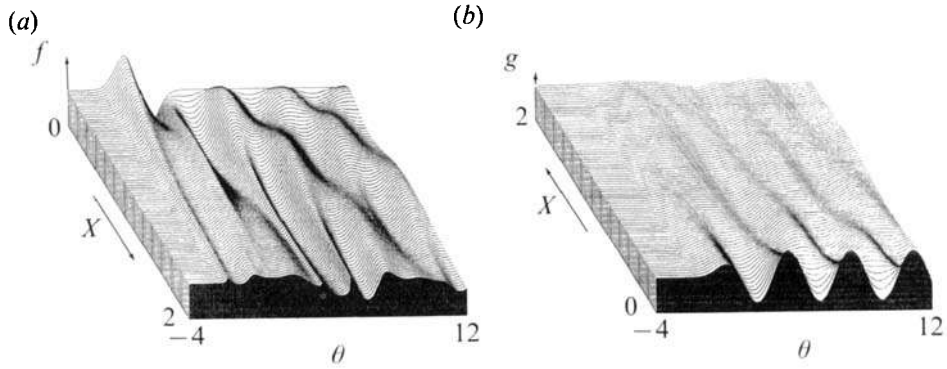

FIGURE 15. Spatial evolutions from a pair of positive and negative pulses for f up to $X = 2$ where (a) and (b) show the evolution of f and g, respectively, for $\delta_R = 0.1$, $\delta_r = 0.01$, $K = 1$ and $\Omega = 3$ and the length of the vertical arrows measures unity of f and g.

Whitham 1974; Drazin & Johnson 1989). As the width of the soliton in θ is proportional to the square root of $K/\alpha\Omega$, the greater value of Ω corresponds to the narrower width so that the pulsive behaviour becomes prominent. Because of the well-known persistent properties of the soliton, such a sharp pulse may be unfavourable from a similar viewpoint of suppression of shock waves, but it is interesting in its own right that the propagation of an acoustic soliton can be realized generally in a pipe with an array of Helmholtz resonators.

To conclude this paper, some problems are mentioned. The magnitude of nonlinearity ϵ has been assumed to be moderately small so that the response of the resonator may be well described by the linear theory. As is shown in the Appendix, this approximation is valid for $\epsilon(A/L_e\Omega)^2 \ll 1$. As ϵ becomes large, the nonlinear response, especially nonlinear loss, will be enhanced, so how this loss plays an additional role in suppression of shock waves is worth examining. This is discussed in Sugimoto (1992).

In the present formulation, the resonators have been regarded as being continuously distributed axially on the assumption that the spacing is much smaller than a characteristic wavelength. However, for a wave of such high-frequency that its wavelength becomes comparable with the spacing, a problem arises of the interaction between neighbouring resonators. In particular, when the wavelength becomes equal to the spacing, the interference resonance might occur (Monkewitz 1985).

Further, if a shock wave is propagated, obviously, the continuum approximation for the resonators breaks down. Even if the second-order derivative in (2.28) is taken into account, a shock thickness is extremely thin and is estimated to be $\beta a_0/\omega$ (Sugimoto 1991). The breaking of approximation might lead one to consider that the shock wave will be reflected or diffracted strongly at each orifice of the resonator, but it should be emphasized that V/Ad has been assumed to be small and comparable with ϵ, as the definition of K in (2.30) implies. Therefore, even if a shock wave emerges, its reflection still remains small. In addition, since the resonators behave as if dormant for the shock wave, this acts favourably for the present approximation and the diffraction is also considered small. Yet it is true, strictly speaking, that the continuum approximation is still invalid around the orifices locally. Even without the array of resonators, the same invalidness happens near the tunnel wall where the shock wave touches.

As ϵ becomes large (though keeping $\epsilon \ll 1$), however, V/Ad should be taken to be proportionally large in order to choose K, for example, to be 10. Then the presence of each resonator tends to be no longer small for the tunnel so that the reflection or the diffraction will happen. This situation now invalidates the basic assumption of the quasi-one-dimension for the main flow in the tunnel. At present, how this effect of finite spacing will affect propagation along a tunnel is an open question.

The author wishes to thank Professor Kakutani for his comments on reading the manuscript.

Appendix. Nonlinear theory for the response of the resonator

The main text has been concerned only with the linear theory for the response of the resonator. In this Appendix, we shall extend it to include the quadratically nonlinear effects. As yet, we still maintain the incompressible approximation in the throat because this validity is endorsed by the assumption $(L/\Lambda)^2 \ll 1$. In order to take account of the loss into turbulence, the momentum flux density in (2.16) must be carefully evaluated.

Before that, it is appropriate to refer to the experimental observations for the flow in the throat (Ingard & Labate 1950; Ingard 1953; Ingard & Ising 1967; Zinn 1970). As the amplitude of the oscillatory flow becomes large, the flow pattern just before entering one orifice and after leaving the other orifice is substantially different. At the inflow side, the gas is sucked in omni-directionally, although bounded locally by the infinite tunnel wall, whereas, at the outflow side, it forms the axial jet on leaving the orifice, entailing a vortex ring. If, therefore, a control volume between $z = 0$ and $z = L$ is extended to just a little upstream of the entrance of one orifice, say at $z = -h$, for a flow directed from the tunnel to the cavity (see figure 2), the point at $z = -h$ may well be regarded as stagnant so that the axial momentum there may be neglected compared with that in the jet leaving the other orifice (Zinn 1970). Then the difficult problem of how far h should be taken arises. In the present context, it must be determined experimentally.

For a cycle when the flow in the throat is directed from the tunnel into the cavity, integration of (2.16) from the stagnation point at $z = -h$ to the exit at $z = L$ leads to

$$L_e \partial q/\partial t = -p_2 + p_{1s} - \overline{(\rho w^2)}_2 - Fr. \tag{A 1}$$

where $L_e (= L+h)$ is the effective length of the throat and p_{1s} denotes the pressure at $z = -h$, which is assumed equal to p in the tunnel. Within the present quadratic theory, $\overline{(\rho w^2)}_2$ may be approximated as $\overline{[(\rho w)^2/\rho]} \approx q^2/\rho_0$. For a cycle of the flow directed from the cavity into the tunnel, on the other hand, the stagnation point is now taken symmetrically at $z = L+h$ and $\overline{(\rho w^2)}_{2s}$ is neglected in comparison with $\overline{(\rho w^2)}_1$. For this approximation, we refer to the paper by Wijngaarden (1968). For an orifice into infinite space, the above result is also obtained by using the boundary conditions due to Wijngaarden.

When q in (A 1) is eliminated by (2.14), q in (2.14) should now be specified up to the quadratic term in p'_c by using the adiabatic relation as follows:

$$q = \frac{V}{B}\frac{\partial \rho_c}{\partial t} = \frac{V}{Ba^2}\frac{\partial p_c}{\partial t} = \frac{V}{Ba_0^2}\left(1 - \frac{\gamma-1}{\gamma}\frac{p'_c}{p_0} + \dots\right)\frac{\partial p'_c}{\partial t}. \tag{A 2}$$

Assuming $p'_c = p'_2$, (2.23) is now replaced by the nonlinear equation:

$$\frac{\partial^2 p'_2}{\partial t^2} + \frac{2L\nu^{\frac{1}{2}}}{L_e r}\frac{\partial^{\frac{3}{2}} p'_2}{\partial t^{\frac{3}{2}}} + \omega_e^2 p'_2 - \frac{\gamma-1}{2\gamma p_0}\frac{\partial^2 p'^2_2}{\partial t^2} + \frac{V}{BL_e\rho_0 a_0^2}\left|\frac{\partial p'_2}{\partial t}\right|\frac{\partial p'_2}{\partial t} = \omega_e^2 p'_1, \tag{A 3}$$

where $\omega_e^2 (= Ba_0^2/L_e V)$ is the natural angular frequency of the resonator taking account of the effective length of the throat. According to Ingard (1953), L in the coefficient of the derivative of order $\frac{3}{2}$ should be lengthened effectively to $L'(= L + 2r)$ to include the viscous end correction. In terms of g, finally, (2.29) is specified up to the quadratic terms as follows:

$$\frac{\partial^2 g}{\partial\theta^2} + \frac{2L'\nu^{\frac{1}{2}}}{L_e r}\frac{\partial^{\frac{3}{2}} g}{\partial\theta^{\frac{3}{2}}} + \Omega g = \Omega f + \epsilon\left[\left(\frac{\gamma-1}{\gamma+1}\right)\frac{\partial^2 g^2}{\partial\theta^2} - \frac{2V}{(\gamma+1)BL_e}\left|\frac{\partial g}{\partial\theta}\right|\frac{\partial g}{\partial\theta}\right], \tag{A 4}$$

where $\Omega = (\omega_e/\omega)^2$ and $2V/(\gamma+1)BL_e = 2(\Lambda/L_e\Omega)^2/(\gamma+1)$ with $\Lambda = a_0/\omega$. Since Λ is much longer than L_e, the nonlinear loss may be negligible as far as $\epsilon(\Lambda/L_e\Omega)^2 \ll 1$. As ϵ becomes large, the nonlinear loss tends to be enhanced, especially for a small value of Ω.

REFERENCES

Chester, W. 1964 Resonant oscillations in closed tubes. *J. Fluid Mech.* **18**, 44–64.

Drazin, P. G. & Johnson, R. S. 1989 *Solitons: An Introduction.* Cambridge University Press.

Ingard, U. 1953 On the theory and design of acoustic resonators. *J. Acoust. Soc. Am.* **25**, 1037–1061.

Ingard, U. & Ising, H. 1967 Acoustic nonlinearity of an orifice. *J. Acoust. Soc. Am.* **42**, 6–17.

Ingard, U. & Labate, S. 1950 Acoustic circulation effects and the nonlinear impedance of orifices. *J. Acoust. Soc. Am.* **22**, 211–218.

Keller, J. J. 1981 Propagation of simple non-linear waves in gas filled tubes with friction. *Z. angew. Math. Phys.* 1932, 170–181.

King, L. V. 1936 On the electrical and acoustic conductivities of cylindrical tubes bounded by infinite flanges. *Phil. Mag.* **21** (7), 128–144.

Lighthill, M. J. 1956 Viscosity effects in sound wave of finite amplitude. In *Surveys in Mechanics* (ed. G. K. Batchelor & R. M. Davies), pp. 250–351. Cambridge University Press.

Monkewitz, P. A. 1985 The response of Helmholtz resonators to external excitation. Part 2. Arrays of slit resonators. *J. Fluid Mech.* **156**, 151–166.

Monkewitz, P. A. & Nguyen-Vo, N.-M. 1985 The response of Helmholtz resonators to external excitation. Part 1. Single resonators. *J. Fluid Mech.* **151**, 477–497.

Pierce, A. D. 1981 *Acoustics: An Introduction to its Physical Principles and Applications.* McGraw-Hill.

Sugimoto, N. 1989 'Generalized' Burgers equations and fractional calculus. In *Nonlinear Wave Motion* (ed. A. Jeffrey), pp. 162–179. Longman.

Sugimoto, N. 1990 Evolution of nonlinear acoustic waves in a gas-filled pipe. In *Frontiers of Nonlinear Acoustics, 12th Intl Symp. on Nonlinear Acoustics* (ed. M. F. Hamilton & D. T. Blackstock), pp. 345–350. Elsevier.

Sugimoto, N. 1991 Burgers equation with a fractional derivative; hereditary effects on nonlinear acoustic waves. *J. Fluid Mech.* **225**, 631–653.

Sugimoto, N. 1992 Suppression of acoustic shock waves in a tunnel by an array of Helmholtz resonators. In *Proc. DGLR/AIAA Aeroacoustic conference, Aachen, Germany*, pp. 571–575. Bonn: DGLR.

Whitham, G. B. 1974 *Linear and Nonlinear Waves.* Wiley-Interscience.

Wijngaarden, L. van 1968 On the oscillations near and at resonance in open pipes. *J. Engng Maths* **2**, 225–240.

Zinn, B. T. 1970 A theoretical study of non-linear damping by Helmholtz resonators. *J. Sound Vib.* **13**, 347–356.